Open access • Journal Article • DOI:10.3171/2011.10.FOCUS11248

Transcranial magnetic resonance imaging-guided focused ultrasound: noninvasive central lateral thalamotomy for chronic neuropathic pain. — Source link

Daniel Jeanmonod, Beat Werner, A. Morel, Lars Michels ...+3 more authors

Institutions: University of Zurich, Boston Children's Hospital, Insightec

Published on: 01 Jan 2012 - Neurosurgical Focus (American Association of Neurological Surgeons)

Topics: Magnetic resonance imaging, Thalamotomy and Neuropathic pain

Transcranial magnetic resonance imaging-guided focused ultrasound: noninvasive central lateral thalamotomy for chronic neuropathic pain

Jeanmonod, D ; Werner, B ; Morel, A ; Michels, Lars ; Zadicario, E ; Schiff, G ; Martin, E

Abstract: Object Recent technological developments open the field of therapeutic application of focused ultrasound to the brain through the intact cranium. The goal of this study was to apply the new transcranial magnetic resonance imaging-guided focused ultrasound (tcMRgFUS) technology to perform noninvasive central lateral thalamotomies (CLTs) as a treatment for chronic neuropathic pain. Methods In 12 patients suffering from chronic therapy-resistant neuropathic pain, tcMRgFUS CLT was proposed. In 11 patients, precisely localized thermal ablations of 3-4 mm in diameter were produced in the posterior part of the central lateral thalamic nucleus at peak temperatures between 51°C and 64°C with the aid of real-time patient monitoring and MR imaging and MR thermometry guidance. The treated neuropathic pain syndromes had peripheral (5 patients) or central (6 patients) origins and covered all body parts (face, arm, leg, trunk, and hemibody). Results Patients experienced mean pain relief of 49% at the 3-month follow-up (9 patients) and 57% at the 1-year follow-up (8 patients). Mean improvement according to the visual analog scale amounted to 42% at 3 months and 41% at 1 year. Six patients experienced immediate and persisting somatosensory improvements. Somatosensory and vestibular clinical manifestations were always observed during sonication time because of ultrasound-based neuronal activation and/or initial therapeutic effects. Quantitative electroencephalography (EEG) showed a significant reduction in EEG spectral overactivities. Thermal ablation sites showed sharply delineated ellipsoidal thermolesions surrounded by short-lived vasogenic edema. Lesion reconstructions (18 lesions in 9 patients) demonstrated targeting precision within a millimeter for all 3 coordinates. There was 1 complication, a bleed in the target with ischemia in the motor thalamus, which led to the introduction of 2 safety measures, that is, the detection of a potential cavitation by a cavitation detector and the maintenance of sonication temperatures below 60°C. Conclusions The authors assert that tcMRgFUS represents a noninvasive, precise, and radiation-free neurosurgical technique for the treatment of neuropathic pain. The procedure avoids mechanical brain tissue shift and eliminates the risk of infection. The possibility of applying sonication thermal spots free from trajectory restrictions should allow one to optimize target coverage. The real-time continuous MR imaging and MR thermometry monitoring of targeting accuracy and thermal effects are major factors in optimizing precision, safety, and efficacy in an outpatient context.

DOI: https://doi.org/10.3171/2011.10.FOCUS11248

Jeanmonod, D; Werner, B; Morel, A; Michels, Lars; Zadicario, E; Schiff, G; Martin, E (2012). Transcranial magnetic resonance imaging-guided focused ultrasound: noninvasive central lateral thalamotomy for chronic neuropathic pain. Neurosurgical Focus, 32(1):E1.
DOI: https://doi.org/10.3171/2011.10.FOCUS11248

Neurosurg Focus 32 (1):E1, 2012

Transcranial magnetic resonance imaging–guided focused ultrasound: noninvasive central lateral thalamotomy for chronic neuropathic pain

Daniel Jeanmonod, M.D.,[1,2] Beat Werner, M.Sc.,[3] Anne Morel, Ph.D.,[1,4] Lars Michels, Ph.D.,[1,3] Eyal Zadicario, M.Sc.,[5] Gilat Schiff, B.Sc.,[5] and Ernst Martin, M.D.[3]

[1]Department of Functional Neurosurgery and [4]Center for Clinical Research, University Hospital Zürich; [2]Center of Ultrasound Functional Neurosurgery, Solothurn; [3]MR-Center, University Children's Hospital, Zürich, Switzerland; and [5]InSightec, Ltd., Tirat Carmel, Israel

Object. Recent technological developments open the field of therapeutic application of focused ultrasound to the brain through the intact cranium. The goal of this study was to apply the new transcranial magnetic resonance imaging–guided focused ultrasound (tcMRgFUS) technology to perform noninvasive central lateral thalamotomies (CLTs) as a treatment for chronic neuropathic pain.

Methods. In 12 patients suffering from chronic therapy-resistant neuropathic pain, tcMRgFUS CLT was proposed. In 11 patients, precisely localized thermal ablations of 3–4 mm in diameter were produced in the posterior part of the central lateral thalamic nucleus at peak temperatures between 51°C and 64°C with the aid of real-time patient monitoring and MR imaging and MR thermometry guidance. The treated neuropathic pain syndromes had peripheral (5 patients) or central (6 patients) origins and covered all body parts (face, arm, leg, trunk, and hemibody).

Results. Patients experienced mean pain relief of 49% at the 3-month follow-up (9 patients) and 57% at the 1-year follow-up (8 patients). Mean improvement according to the visual analog scale amounted to 42% at 3 months and 41% at 1 year. Six patients experienced immediate and persisting somatosensory improvements. Somatosensory and vestibular clinical manifestations were always observed during sonication time because of ultrasound-based neuronal activation and/or initial therapeutic effects. Quantitative electroencephalography (EEG) showed a significant reduction in EEG spectral overactivities. Thermal ablation sites showed sharply delineated ellipsoidal thermolesions surrounded by short-lived vasogenic edema. Lesion reconstructions (18 lesions in 9 patients) demonstrated targeting precision within a millimeter for all 3 coordinates. There was 1 complication, a bleed in the target with ischemia in the motor thalamus, which led to the introduction of 2 safety measures, that is, the detection of a potential cavitation by a cavitation detector and the maintenance of sonication temperatures below 60°C.

Conclusions. The authors assert that tcMRgFUS represents a noninvasive, precise, and radiation-free neurosurgical technique for the treatment of neuropathic pain. The procedure avoids mechanical brain tissue shift and eliminates the risk of infection. The possibility of applying sonication thermal spots free from trajectory restrictions should allow one to optimize target coverage. The real-time continuous MR imaging and MR thermometry monitoring of targeting accuracy and thermal effects are major factors in optimizing precision, safety, and efficacy in an outpatient context.

(http://thejns.org/doi/abs/10.3171/2011.10.FOCUS11248)

Key Words • central lateral thalamotomy • neuropathic or neurogenic pain • transcranial magnetic resonance imaging–guided focused ultrasound

Considering the inherent risks related to neurosurgical procedures, such as infections and hemorrhages, there is an obvious demand for less invasive alternative procedures. Following extensive preclinical investigations,[4–8,10,11,13,15,24,25,31,32] a clinically relevant prototype of a tcMRgFUS device for thermal ablation was developed.[9,12,14] Because of its noninvasiveness, focused ultrasound technology eliminates the risk of infection, reduces the risk of bleeding, and limits collateral damage to nontargeted tissue. Magnetic resonance imaging allows precise intraprocedural localization of the ablation target, definition and verification of safety margins for the ultrasound treatment, real-time monitoring of thermal ablation dynamics, and intra- and posttreatment assessment of intervention results.[2,3,21] The tcMRgFUS technique involves the transformation of sonic into thermal energy and the production of a thermolesion. The possibility of

Abbreviations used in this paper: CLp = posterior part of the thalamic central lateral nucleus; CLT = central lateral thalamotomy; DT = diffusion tensor; EEG = electroencephalography; tcMRgFUS = transcranial magnetic resonance imaging–guided focused ultrasound; VAS = visual analog scale; VLp = posterior part of the thalamic motor ventral lateral nucleus.

applying this technique transcranially (that is, without injury to skin and skull) has great potential in the field of neurosurgery.[16,22]

A recent landmark clinical study[23] examined the feasibility and initial technical results of tcMRgFUS and showed for the first time in 3 patients that it is possible to focus the ultrasound beam through the intact skull into the brain and to visualize internal heating at the focal point and on the brain surface by using MR imaging temperature mapping. These findings constitute a significant step forward in establishing an entirely noninvasive alternative therapy to surgery for brain disorders.

Based on our long-term clinical experience in functional neurosurgery for neuropathic (or neurogenic) pain with radiofrequency stereotactic interventions in the medial thalamus,[17,19,20] and after preclinical studies with phantoms, biological tissues, and ex vivo human head preparations, we adapted our interventional procedure to perform CLTs in patients suffering from chronic neuropathic pain using the tcMRgFUS technology. The study was approved by the ethics committee of Zurich University and the state of Zurich (Kantonale Ethikkommission des Kantons Zürich). An initial report about the short-term results for 9 patients has already been published.[26] The present report provides clinical and neurophysiological results over 1 year as well as analyses of the targeting precision and the postoperative MR imaging visualization of the produced thermolesions.

Methods

Patient Population

Twelve patients with chronic therapy-resistant neuropathic pain were enrolled for tcMRgFUS CLT and provided their written informed consent. For the sake of safety, a thermal spot of only 42°C was placed in the first patient. This intervention did not result in a thermolesion and this patient was excluded from further analysis. Therapy resistance was established based on the lack of efficacy and/or the side effects of antiepileptic and antidepressant drugs. Patients were 45–75 years old and suffered from facial pain (3 patients), thoracic pain (1 patient), lower-extremity pain (3 patients), upper-extremity pain (4 patients), and hemibody pain (1 patient), of central (6 patients) or peripheral (5 patients) origin (Table 1). The causal lesions at the origin of the different neuropathic pain syndromes were amputation (phantom limb pain, 1 patient), root compression in failed–back surgery syndrome (1 patient), root compression by neurinoma (1 patient), herpes zoster infection (1 patient), nerve trauma (1 patient), spinal cord lesion (2 patients), putaminal lesion (1 patient), brachial plexus avulsion (2 patients), and thalamic infarct (1 patient). The duration of pain before treatment was between 1.5 and 21 years (mean 8.5 years). A pre- and postoperative pain assessment was performed using a detailed questionnaire, including the items of the McGill Pain Questionnaire. The VAS rating of pain intensity was noted for the least and worst pain intensities on a scale between 1 and 100. In addition, patients provided a global percentage value of postoperative pain relief as compared with the preoperative state. In patients with chronic therapy-resistant neuropathic pain, a pain relief scale and VAS value comparisons for pain intensity reduction after treatment are the most adapted and commonly recognized assessment indicators to serve as primary outcome measures for success. Patients were clinically examined as follows: repetitive assessments during the treatment (see below); clinical examination on the evening of the treatment day and 24 and 48 hours afterward; telephone consultation at 1 month after treatment; and full reassessment at 3 months and 1 year after treatment.

Prior to treatment, the patients underwent CT scanning (512 × 512 matrix, 1-mm slice thickness) that covered the entire cranium as well as an MR imaging examination with T1- and T2-weighted images and DT imag-

TABLE 1: Summary of clinical and treatment data in 11 patients who underwent tcMRgFUS*

Case No.	Duration of Pain (yrs)	Location of Pain	Cause of Pain	CLT Side	Max Temp at Target (°C)	Sensory Improvements	Activation Effects
1	6	leg	root compression (disc herniation)	lt/rt	53	+	paresthesias in leg
2	8.5	hemibody	thalamic infarct	lt	51	+	vestibular, pain in head
3	2.5	face	traumatic trigeminal nerve injury	rt†	57	+	vestibular, pain in face
4	1.5	face	striatal	rt	59	−	vestibular, nausea, paresthesias in face, pain in face
5	4	face	postherpetic neuralgia	lt/rt	55	+	absent
6	9	arm	root compression (neurinoma)	lt/rt†	58	+	vestibular, vomiting, pain in head
7	17	arm	avulsion of brachial plexus	lt/rt†	57	−	vestibular, pain in head, paresthesias in arm
8	8	leg	phantom leg pain	rt†	55	−	pain in head
9	16	arms & legs	paraplegia	lt/rt	60	−	vestibular, pain in leg
10	7	thorax	syringomyelia	lt/rt	64	+	vestibular, pain in head, nausea
11	21	arm	avulsion of brachial plexus	lt	64	−	vestibular, paresthesias, pain in head

* The mean duration of pain among the patients was 8.5 years. Neurological deficits occurred in only one patient (Case 11): neglect and dysmetria because of bleeding and ischemia. Abbreviation: Temp = temperature ; + = improvement; − = no change.
† Complement to radiofrequency CLT.

ing. Identical MR imaging series were obtained at 2 days, 3 months, and 1 year postsonication.

Surgical Procedure

The treatment was performed in a 3-T MR imaging system (Signa HDx, GE) using the ExAblate 4000 device (InSightec), which features a 30-cm-diameter hemispherical 1024 element phased-array transducer operating at 650 kHz and held by a mechanical positioner. Magnetic resonance imaging was performed using an 8-channel torso phased-array coil.

The patient's scalp was fully and closely shaved, and the head was immobilized by fixation in an MR imaging–compatible frame (Radionics; Fig. 1). A circular flexible silicone membrane with a central hole was stretched around the patient's head and sealed to the outer face of the transducer to contain the degassed and chilled (15°–20°C) water that was circulated in the area between the head and the transducer. This membrane is tight enough to prevent water leakage without preventing blood circulation to the scalp.

Axial and sagittal T1- and T2-weighted fast spin echo images were obtained and coregistered to the previously acquired MR and CT images and to the current MR imaging/transducer coordinates. These images allowed us to calibrate the system and to produce precise stereotactic planes for target determination. The target area, the CLp, was localized on 3D T1-weighted MR images using the stereotactic multiarchitectonic Morel atlas of the human thalamus and basal ganglia.[27] The coordinates of the targets were then entered into the planning software of the tcMRgFUS system.

Several low-power sonications of 10–20 seconds duration were applied to induce peak temperatures of 39°–42°C, known to be below the ablation threshold. They allowed us to assess the exact position and size of the thermal spot and the overall safety profile of the applied sonication parameters.[15] Several high-power sonications were then applied in an iterative process guided by MR imaging and MR thermometry, with stepwise increases in the acoustic power and energy to finally achieve a peak temperature at the target between 51°C and 64°C (Fig. 2). The final peak temperature in each treatment is an outcome of various factors. Thermocoagulation effects on tissue can be produced and visualized from 50°C and up, with a 100% necrosis considered to arise at 55°–57°C. Optimal coverage of the target and the clinical feedback from patients both play a role in determining the final peak temperatures. These factors explain their range between 55°C and 64°C for the 9 patients with complete lesioning (see C*linical Results*). Typically, we applied sonications of 10 to 20 seconds in duration with up to a maximum acoustic power of 1200 and 800 W, respectively, corresponding to 12,000 J per sonication. The mean peak focal temperature achieved in the treatments was 53 ± 3.3°C (range 48°–61°C).

Fig. 1. Photograph of a patient ready for the sonication. The head is immobilized in a stereotactic frame. The transducer is held and positioned by a mechanical positioning system. The silicone membrane seals the space between the patient's head and the transducer, which is filled by degassed, cooled, and circulated water.

Patients were fully awake and responsive during all stages of the intervention. The only medication administered before the procedure consisted of lorazepam 2.5 mg orally. In 2 patients, a subcutaneous opiate injection was necessary because of back pain due to a motionless supine position on the MR imaging table for an extended period of time. During the entire series of sonications, patients were examined and questioned repeatedly to ensure their neurological integrity and to assess 1) changes in pain qualities, extension, and intensity; 2) potential somatosensory improvements; 3) the appearance of somatosensory, vestibular, and vegetative manifestations experienced during the treatment; and 4) the absence of any motor or somatosensory deficit.

The CLT was performed unilaterally (contralateral to the pain location) in 5 patients and bilaterally in 6 patients. A bilateral CLT is, in general, necessary, and it is as sparing of brain functions as a unilateral one.[19] In 4 patients, the tcMRgFUS treatment complemented a previously performed radiofrequency treatment. The CLT was performed unilaterally for the following reasons: complement to radiofrequency treatment (2 patients), appearance of bleeding (1 patient; see *Clinical Results*), immediate 100% pain relief after treatment of the first side (1 patient), and intolerance of a longer intervention time (1 patient).

Target Reconstruction Method

To evaluate the accuracy of tcMRgFUS targeting, the 3D coordinates of the centers of the sonication lesions, outlined on T2-weighted MR images obtained 48 hours after sonication, were measured and compared with presurgical stereotactic coordinates of the ablation targets. The dorsoventral coordinates were determined by the distance from the anterior commissure–posterior commissure plane passing through the center of the anterior and posterior commissures (on sagittal and/or coronal MR imaging); the anteroposterior coordinates, by the distance from the posterior commissure (on axial and sagittal MR imaging); and the mediolateral coordinates, by the distance from the thalamoventricular border (on coronal and axial MR imaging).

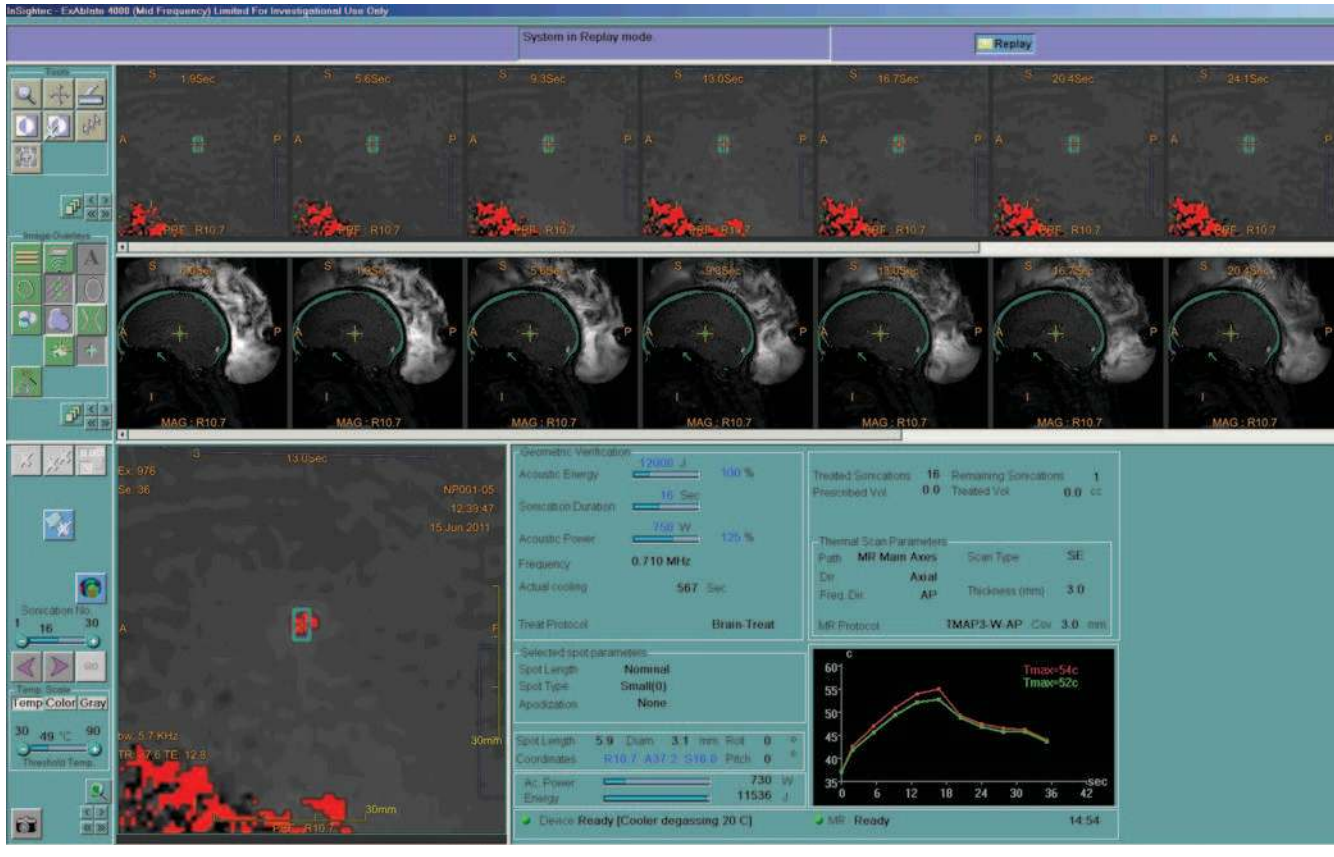

Fig. 2. Screenshot of the ExAblate 4000 display showing a series of proton resonance frequency MR images (obtained every 3.7 seconds, **upper**) and a series of magnitude images **(center)**. Magnification of a proton resonance frequency picture **(lower left)** showing in the center a thermal spot centered in the calculated target display *(blue rectangle)*. Display **(lower right)** showing the applied acoustic energy, sonication duration, acoustic power, target coordinates, thermal scan parameters, and temperature curve.

Quantitative EEG Procedure

Electroencephalography recording was performed at the time of clinical assessment, before entry into the study. The clinical states of the patients, reassessed at the time of enrollment in the month before treatment, remained unchanged, requiring no repetition of EEG recordings. A 10-minute EEG recording was monitored during alternating eyes-open and eyes-closed states (2 blocks with eyes open and 2 blocks with eyes closed). The EEG activity was recorded from a cap with 60 scalp channels (Easycap) using a 500-Hz sampling rate, 32-mV input range, and 0.1- to 250-Hz bandpass filters. The impedance was kept below 20 kΩ. Electrodes were mounted according to the 10–20 system plus the following 10–10 system sites: FPz, AFz, FCz, CPz, POz, Oz, Iz, F5/6, FC1/2/3/4/5/6, FT7/8/9/10, C1/2/5/6, CP1/2/3/4/5/6, TP7/8/9/10, P5/6, PO1/2/9/10, OI1/2. Both O1/2 and FP1/2 were placed 2 cm laterally from the standard positions for more even coverage. Note that F1 served as the recording reference and F2 was the ground electrode. Two additional electrodes were placed below the outer canthus of each eye to measure for electrooculography.

BrainVision Analyzer software (version 1.05, Brain Products) served for offline processing of the EEG. Subsequently, electrooculography channels were discarded from further analysis. Data were digitally bandpass filtered (0.5–70 Hz, 24 dB/oct, and 50-Hz notch) and downsampled to 250 Hz. An infomax independent component analysis was calculated to remove artifacts related to eye movements, eye blinks, and muscle contractions. Movement-related artifacts, which may not be suitable for independent component analysis correction, were excluded from the unmixing procedure. Components were profiled by their topography, activation time course, and spectrogram. After artifact removal, the components were first back-projected to the EEG and then transformed to the average reference. Segments with remaining artifacts were marked and excluded from successive analysis (mean length of the EEG was about 4 minutes for each resting state condition). Next, the data were parsed into 2-second epochs. Absolute spectral power was estimated for each epoch using fast Fourier transform (Hanning window: 10%, zero-padded, resolution 0.5 Hz). The mean spectral band power was calculated from 1–48 Hz. Spectral bands were defined as follows: delta (2–4 Hz), theta (4–8 Hz), alpha1 (8–13 Hz), and beta (13–30 Hz). (Note that the superior spectral band limit is included only in the next higher band.) The EEG was analyzed in terms of absolute spectral power as well as electrode-wise comparisons to preserve topographic information (topoplots). For each separate condition, spectral power values were averaged across fast Fourier transform epochs and aver-

aged within the above frequency bands. Group means were compared using t-statistics ($p < 0.05$ indicated significance).

Results

Clinical Results

In the first 2 patients of this series, the therapeutic lesions placed in the CLp, as seen 48 hours after treatment on T2-weighted and DT images, were too small to cover it in any sufficient manner. The tcMRgFUS treatment could thus be considered complete in only 9 of the 11 patients. An analysis of global pain relief percentages as reported by the patients and of VAS values was performed for these 9 patients only; results are listed in Table 2. The preoperative mean VAS score was 59.5/100. Significant pain relief (mean group value 55%) was already reported during and at the end of the procedure. More reliable pain relief percentages were collected at 2 days (mean group value 71.1%, 9 patients), 3 months (mean group value 49.4%, 9 patients), and 1 year (mean group value 56.9%, 8 patients) after treatment. The postoperative mean VAS score was 34.3/100 at 3 months and 35.3/100 at 1 year, representing a 42.3% and 40.7% postoperative improvement, respectively.

At the 1-year follow-up, among 8 patients, 5 took no drugs against pain, but 3 maintained a globally unchanged regimen. Drug intake is, for many reasons, not a good marker of the postoperative evolution of patients who have suffered from long-standing, therapy-resistant neuropathic pain. On the one hand, some patients may have stopped their drug intake before the intervention because of insufficient or absent efficacy or because of side effects. On the other hand, some patients have habituated to their drugs for years and are afraid to reduce or stop them, making a consequent and predetermined drug reduction program practically and ethically impossible.

Six patients experienced significant intraoperative somatosensory improvements in and around the pain area, which they spontaneously mentioned during the treatment. These improvements were confirmed after the intervention and remained at the 3-month and 1-year follow-ups.

Patients reported clinical effects during sonication, such as pain relief (9 patients), vestibular with or without vegetative manifestations (8 patients), paresthesias (4 patients), or dysesthesias/pain (9 patients). These symptoms could already be observed at focal temperatures below 50°C.

In 1 patient, displacement of the headframe occurred, but it was repositioned without negative consequences. In the last minutes of the procedure after all planned sonications had been completed, the last patient in this series experienced the acute appearance of right-sided motor hemineglect with dysmetria of the arm and leg and dysarthria. Magnetic resonance imaging examinations immediately and 48 hours thereafter revealed the presence of a bleed 8–10 mm in maximal diameter centered in the targeted CLp, as well as ischemic changes in the VLp. These were causal for the motor symptoms presented by the patient. Subsequent control MR images showed a good progressive resorption of the bleeding. Clinically, there was a 70%–80% reduction in the motor symptoms over the next 24 hours. With time, all dysmetric manifestations disappeared except during activation of the finer functions of speaking and writing, which at 1 year posttreatment remained impeded during demanding and stressful personal and professional interactions.

Lesion Coordinate Reconstruction for Assessment of Targeting Precision

The sonication lesions were at best visible 48 hours after the intervention (Fig. 3 upper) and consisted of a mostly hyperintense ellipsoid lesion with a diameter of 3–4 mm and a length of 4–5 mm. It was surrounded by a

TABLE 2: Summary of postoperative data in 11 patients who underwent tcMRgFUS*

	Pain Relief (%)				VAS Score (lowest–highest, mean)			
Case No.	Acute	2 Days	3 Mos	1 Yr	Before Sonication	3 Mos After Sonication	1 Yr After Sonication	1 Yr Postop Drug Intake
1	100	70	0	lost to FU	70–80	16–79	UN	reduced†
2	30	30	0–30	lost to FU	72–100	40–70	UN	unchanged
3	10	100	80	80	52–73, 62.5	5–20, 12.5	9–16, 12.5	stopped
4	70	50	50	95	40–80, 60	0–72, 36	9–36, 22.5	stopped
5	100	80	0	deceased‡	12–78, 45	0–50, 25	UN	UN
6	30	100	90	100	39–62, 50.5	0–11, 5.5	0	stopped
7	30	50	50	40	22–85, 53.5	15–84, 49.5	21–86, 53.5	unchanged
8	100	100	70	50	56–85, 70.5	13–80, 46.5	77	unchanged
9	0	10	0	0	67–90, 78.5	54–89, 71.5	11–84, 47.5	unchanged
10	100	75	90	80	44–91, 67.5	0–14, 7	0–28, 14	stopped
11		75	15	10	25–70, 47.5	30–80, 55	30–80, 55	stopped
overall mean§	55	71.1	49.4	56.9	59.5	34.3	35.3	UN

* FU = follow-up; UN = unavailable.
† Includes opiates.
‡ Unrelated medical cause.
§ The mean values for global pain relief and VAS were calculated for Cases 3–11 only.

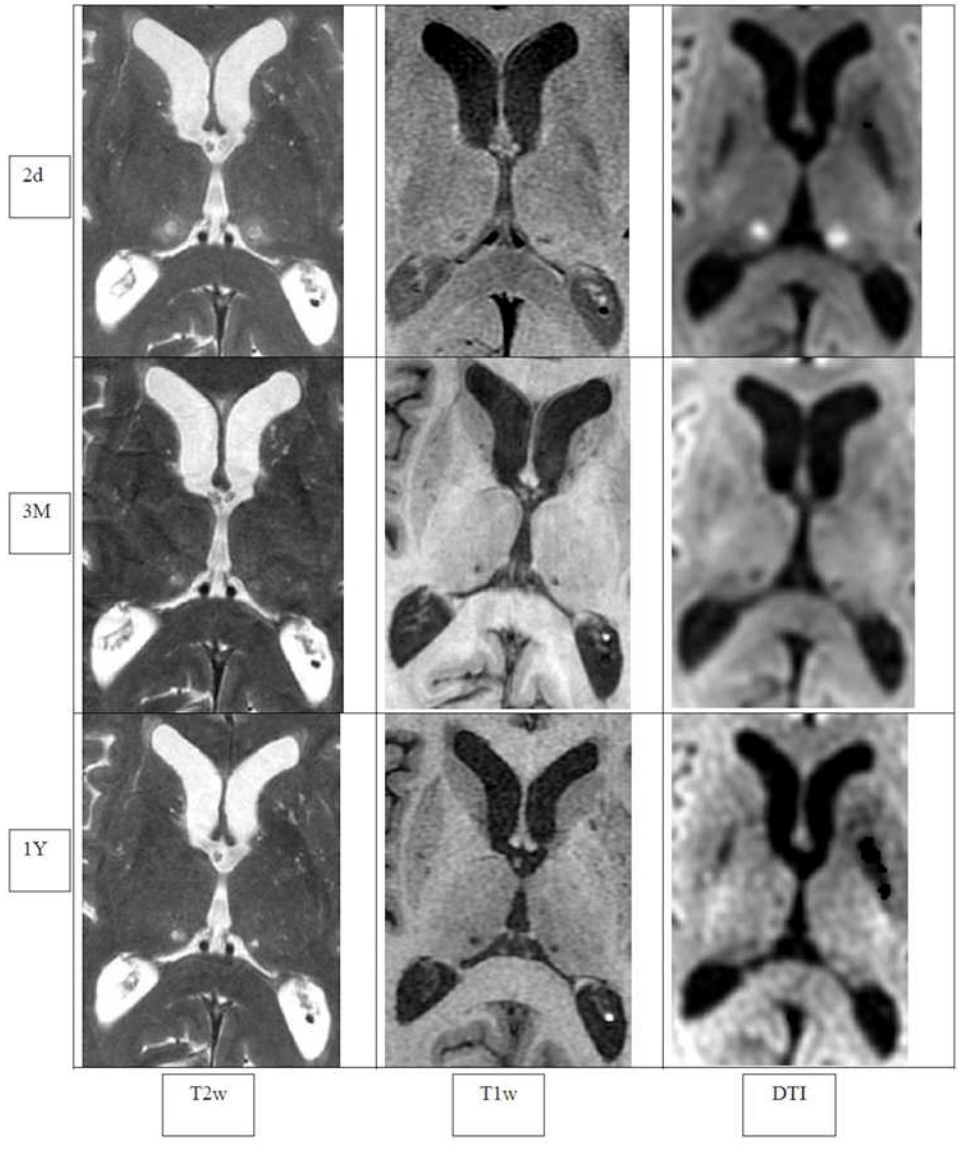

Fig. 3. Magnetic resonance images showing the therapeutic lesions 2 days (2d), 3 months (3M), and 1 year (1Y) after the sonication. DTI = diffusion tensor images, isotropic diffusion mode; T1w = T1-weighted images; T2w = T2-weighted images.

fuzzy and irregularly shaped area of perifocal vasogenic edema, which completely receded over a month. Lesions were significantly smaller at 3 and 12 months after treatment (Fig. 3 center and lower). A detailed neuroradiological description of the sonication lesions was previously published.[26]

The median and mean (± standard deviation) of the targeting accuracy are given in millimeters in Table 3 for the patients in Cases 1–9 and separately for the first and second groups treated sequentially. The deviations for the first group (5 patients, 9 lesions) are larger in all axes than for the second group (4 patients, 9 lesions) treated after the implementation of procedural improvements, that is, better accuracy in the thermal spot realignment during the verification phase at low temperatures, and an optimization of the determination of the center frequency of the MR acquisition for proper thermal imaging projection. The increased accuracy between the 2 subgroups was most marked in the anteroposterior direction (from 1.17 ± 0.58 to 0.39 ± 0.46 mm). The mean values for the whole group are < 1 mm in all axes, but larger in the mediolateral axis than in the other axes.

Localization of the tcMRgFUS lesions in the thalamus is illustrated in Fig. 4. Projections of the lesions onto horizontal sections of the Morel atlas[27] showed the following: of 18 lesions, 7 enclosed most, if not the whole, anteroposterior extent of the CLp (targeted in CLT); 5 enclosed half of it; and 6 enclosed up to one-third. Most partial CLT lesions encroached onto the pulvinar, and only 2 encroached on the posteriormost part of the mediodorsal nucleus. The first series of lesions (Cases 1–5, Subgroup 1) tended to be more posterior and overlapped less with the CLp than the rest of the lesions (Cases 6–9, Subgroup 2). This result corresponds to the measurements shown in Table 3. Note that in the patients in Cases 3, 6, and 7, a part of the excentering of the focused ultrasound lesions

TABLE 3: Precision of tcMRgFUS targeting*

Parameter	Total Patients		Subgroup 1		Subgroup 2	
	Mean ± SD	Median	Mean ± SD	Median	Mean ± SD	Median
no. of patients	9		5		4	
dorsoventral	0.58 ± 0.63	0.5	0.61 ± 0.57	0.5	0.56 ± 0.68	0
anteroposterior	0.78 ± 0.65	1.0	1.17 ± 0.58	1.5	0.39 ± 0.46	0
mediolateral	0.83 ± 0.78	0.5	1.01 ± 0.85	0.7	0.82 ± 0.79	0.5

* Values of dorsoventral, anteroposterior, and mediolateral differences between centers of the sonication lesions and presurgical target coordinates are expressed in mm.

is related to target adaptations due to previously made radiofrequency CLT lesions and not only to suboptimal procedural factors.

Quantitative EEG Assessment

The spectral comparison of the 8 patients who underwent a 3- and 12-month follow-up EEG recording revealed 2 major findings. First, spectral power was elevated in all frequency bands (delta–beta) before the sonication (Fig. 5 upper). Second, frequency band–specific spectral power amplitudes were reduced 3 and 12 months after the sonication, and thus were approaching the spectral curve of healthy volunteers. An electrode-wise comparison of frequency band–specific spectral power showed that several scalp locations displayed significantly elevated power before as compared with 12 months after sonication (Fig. 5 lower). On the topoplots featured in Fig. 5, black dots indicate the electrodes, which show significantly ($p < 0.05$, $t > 2$) higher spectral power before as compared with 12 months after sonication, in delta (2–4 Hz) and theta (4–8 Hz) bands at frontal, centrotemporal, and parietal electrodes; and in alpha (8–13 Hz) and beta (13–30 Hz) bands at centroparietal electrodes.

Discussion

This report on the clinical, neurophysiological, and neuroanatomical results of tcMRgFUS CLT for neuropathic pain demonstrates the precision and efficacy of this surgical approach and confirms the short-term results reported previously.[26]

The clinical results presented here support our long experience with radiofrequency CLT treatment for chronic therapy-resistant neuropathic pain.[19,20] The patients in this series showed a typical mean group pain relief profile across time, from 71% at 2 days after treatment to 49% at 3 months and 57% at 1 year after treatment. The VAS improvement was similar at 3 months (42%) and at 1 year (41%). This profile can be explained as follows: the immediate reduction of low-frequency overactivity using CLT provides the patient with acute relief. However, complex nonlinear systems, like the thalamocortical system, display typically protracted dynamics when they change from one activity level to another and search for a new resting state. This explains why the EEG spectral improvements, in parallel with clinical relief, develop over at least 1 year.[28,30] After the initial pain relief and as the thalamocortical network just begins its retuning (reorganization) toward normal activity, emotional, cognitive, and social factors intervene and influence the patient's evolution as he or she revisits specific personal goals put aside because of chronic pain and progressively adapts to new individual goals and concepts. This endeavor becomes less and less demanding as time goes by and the thalamocortical network comes closer to normality.

Previous studies[28–30] have related the clinical phenomenon of chronic neuropathic pain to an increase in low- and high-frequency spectral EEG and magnetoencephalography activities. This correlation is further supported by the evidence of reduced theta overactivity in the EEG recordings of patients treated with CLT.[28,30] Electroencephalography spectral analysis can thus be used as an additional tool to diagnose chronic neuropathic pain states and monitor their postoperative evolution. The EEG spectral data presented here are fully compatible with these studies and demonstrate 1) EEG overactivities in all frequency domains and 2) their reduction, particularly strong in the beta range, after the tcMRgFUS treatment. They serve as additional evidence in favor of thalamocortical mechanisms being at the source of neuropathic pain.

The absence of postoperative clinical deficits, known for years about medial thalamotomies, has been confirmed for CLT, a medial thalamotomy centered on the CLp where an abnormal low-threshold calcium spike burst activity was recorded.[17] Results in the present study confirm the sparing mode of action of CLT, which selectively targets dysfunctional thalamocortical regulators, initiating a resumption of normal thalamocortical dynamics while sparing all functions supported by unaffected thalamocortical regulators and executors. The absence of postoperative kindling of new neuropathic pain mechanisms has been shown years after CLT and can be related to the selective reduction of the thalamocortical pathophysiology at the source of neuropathic pain phenomena.[19,20] Six patients experienced immediate and significant somatosensory improvements, which persisted at the 3-month and 1-year follow-ups. This result corresponds with observations after radiofrequency lesions[18] and can also be related to the reduction of thalamocortical overactivity by CLT.

Effects during sonication, whether somatosensory, vestibular, or vegetative, were observed in all patients. They may have 2 origins: 1) an activation of neurons during the few seconds before the thermal ablation effect and 2) initial manifestations of the resumption of a more normal thalamocortical dynamics, as is routinely seen in our experience with radiofrequency CLT, thereby indicat-

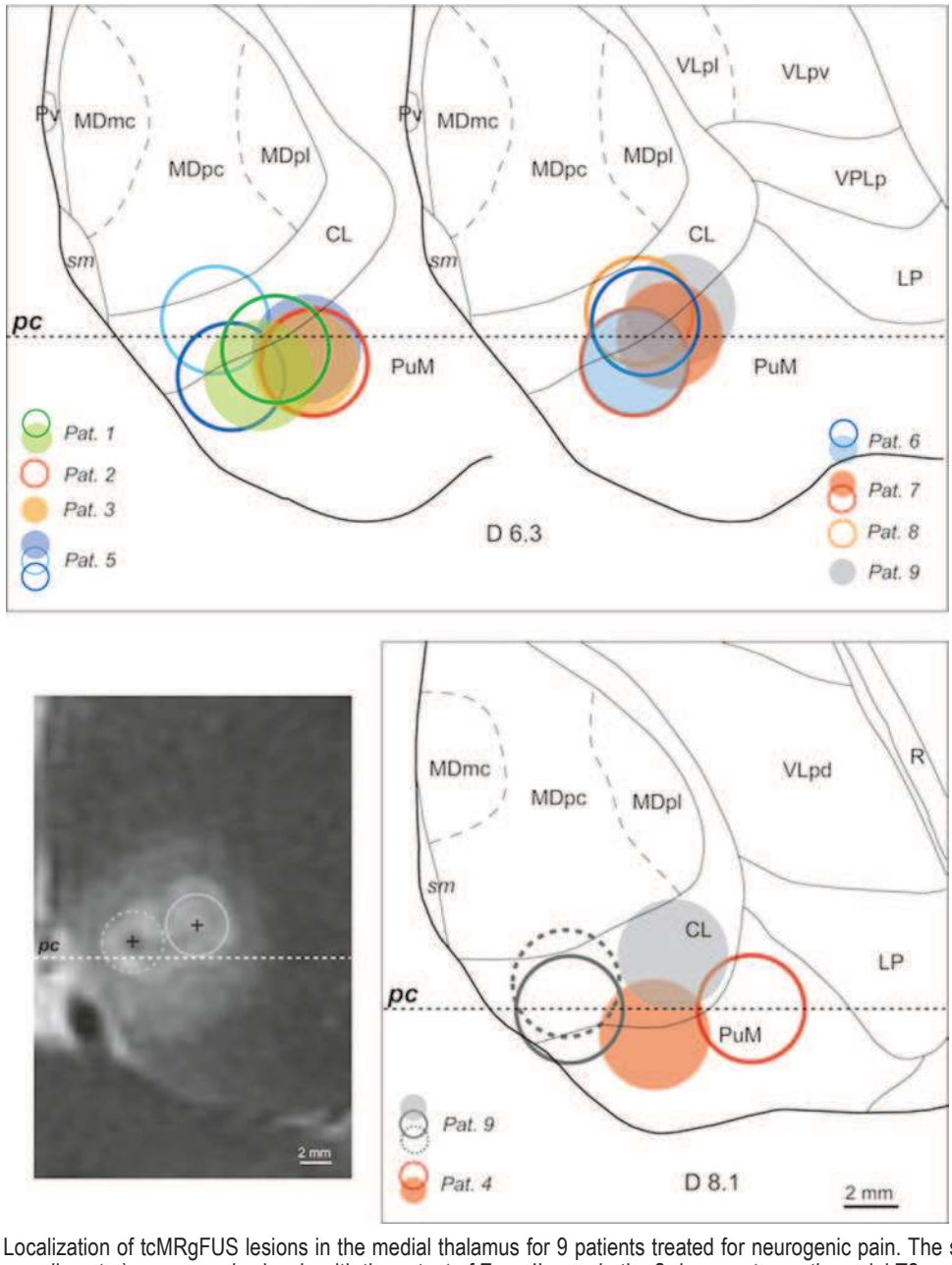

Fig. 4. Localization of tcMRgFUS lesions in the medial thalamus for 9 patients treated for neurogenic pain. The size of the lesions (4-mm diameter) corresponds closely with the extent of Zone II seen in the 2-days postoperative axial T2-weighted MR image **(lower left)**. The location of the lesion in relation to the CLp is determined by projection of the corresponding atlas maps (6.3 **[upper]** and 8.1 **[lower right]** mm dorsal to the intercommissural plane) onto the MR image by using the position of the posterior commissure (pc, *dotted line*) for alignment. The 2 lesions projected on the MR image are the 2 anteriormost lesions in the patient in Case 9 **(lower right)**. CL = central lateral; LP = lateral posterior; MDmc = mediodorsal magnocellular division; MDpc = mediodorsal parvocellular division; MDpl = mediodorsal paralamellar division; PuM = medial pulvinar; Pv = paraventricular; R = reticular thalamic nucleus; sm = stria medullaris; VLpd = ventral lateral posterior, dorsal division; VLpl = ventral lateral posterior, paralamellar division; VLpv = ventral lateral posterior, ventral division; VPLp = ventral posterior lateral, posterior part..

ing appropriate target placement. To monitor safety and acquire real-time feedback and information, the presence of a clinician by the patient's side throughout the treatment phase is required. This practice ensures that the sonication effects, including changes in neurological parameters, as well as patient safety and comfort during the extended period of time in the MR imaging unit are closely monitored.

The tcMRgFUS CLT thermolesions as seen on MR imaging 2 days after sonication were surrounded by a vasogenic edema, which was no longer visible after 1 month. Visualization of the thermolesion itself receded between 1 and 3 months. These observations are indicative of a selective neuronal coagulation with few hemorrhagic components, which are often seen with radiofrequency thermolesions and correlate with a much longer

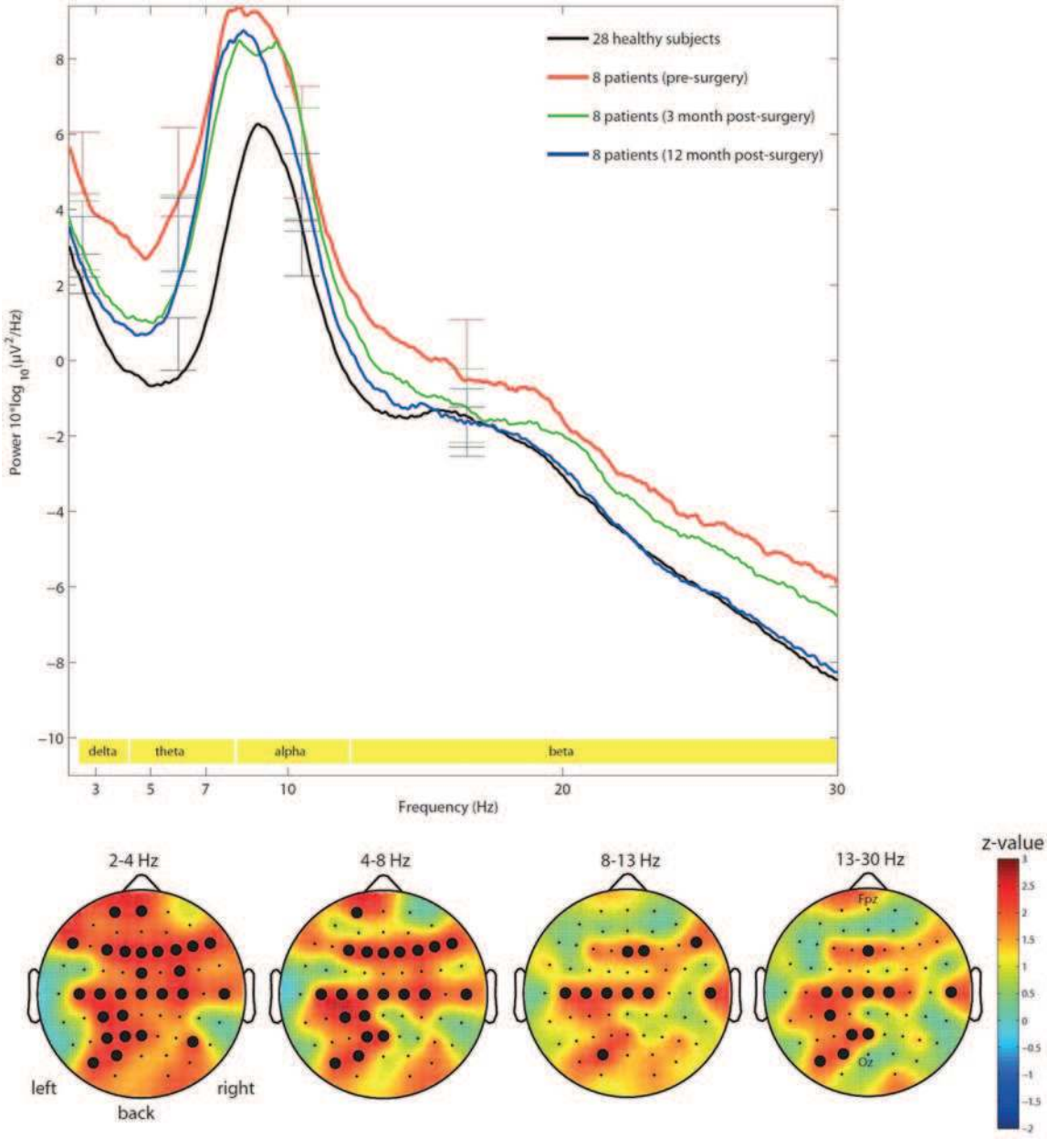

Fig. 5. Upper: Graph showing power spectral curves of the patients before and after surgery with standard deviations of the means *(vertical bars)*. *Black curve* is for controls. Frequency bands are shown in *yellow* at the bottom of the graph. **Lower:** Topoplots showing electrode-wise comparisons. *Black dots* indicate the electrodes, which showed significantly higher spectral power before surgery as compared with 12 months after surgery.

maintenance of edema. With tcMRgFUS, there is no mechanical trauma of the target tissue, and the temperature at the center of the hotspot is not as high as with radiofrequency ablation. With radiofrequency ablation, the temperature, depending on the electrode geometry, must be much higher than 60°C at the electrode tip to achieve the necessary heating over the desired target volume. At 48 hours postsonication, the blood-brain barrier was seen to be closed.[26] All of these observations are compatible with a clean thermolesion displaying a fast healing process and speak against the possibility of unexpected deleterious long-term tissue phenomena. In this context, the bleeding that occurred in our last patient demands an explanation, particularly since he presented no increased risk factors (he had normal blood pressure and coagulation). A detailed case study was performed to analyze the factors that might have facilitated this event. Two factors were considered: first, the possibility of the development of a cavitation effect, although a detailed analysis provided no direct evidence in its favor. Nevertheless, this possibility requires the installation of a cavitation detector to detect and stop this phenomenon as soon as it appears. Second, a temperature-related factor must be considered, supported by published evidence[32] and confirmed by recent experimental data collected in the context of this case study. Accordingly, we recommend maintaining the sonication

temperatures below 60°C. Note that the bleeding itself, centered in the adequately targeted CLp, did not produce deficits. It is the ischemia, extending anteriorly and laterally into the VLp, that caused the typical motor symptomatology. We hypothesize a blood-induced vasospasm in the VLp as a causal link between the 2 events.

Our target reconstructions demonstrate precision within a millimeter for all 3 target coordinates. The classic stereotactic techniques involving penetration of an electrode into the brain cannot, despite adequate technological accuracy, reach such final precision because of the unforeseeable mechanical shift of brain tissue by the electrode.[1] In addition, the tcMRgFUS CLT should allow for optimal target volume coverage thanks to the absence of electrode trajectory restrictions. Such optimization should develop with increased procedural experience and further technological developments, both decreasing the time devoted to optimal target coverage during treatment. This should correlate with higher long-term pain relief scores as compared with our previous results with CLT.[19] The patient group in the present study is too small to be conclusive on this question, and further long-term studies on larger patient groups will have to verify whether this is indeed the case. Sonication also proved to be particularly helpful for 4 patients who had previously been treated with radiofrequency CLT, facilitating the complementary treatment by avoiding potential shifts of penetrations through gliotic tissue.

Conclusions

Results of the current study highlight the precision and efficiency of tcMRgFUS for treating chronic neuropathic pain. The noninvasiveness of the procedure and specifically the continuous MR imaging and MR thermometry monitoring of the intervention represent major factors toward an optimization of safety conditions. This radiation-free technology can be applied to other functional brain disorders as well as to numerous other neurosurgical indications and is an important option because of the elimination of brain tissue shift or trauma during therapy. Besides, tcMRgFUS has a probably reduced bleeding risk, no risk of intracranial infection, and is not limited in target coverage by trajectory constraints.

Disclosure

This work was supported by the University of Zürich, the Swiss Federal Institute of Technology Zürich, the University Children's Hospital Zürich, the Swiss National Center of Competence in Research (NCCR) "Computer Aided and Image Guided Medical Interventions", the Focused Ultrasound Surgery Foundation (Charlottesville, VA), and the Sanitas Hospital in Kirchberg. Mr. Zadicario is an employee of InSightec, Ltd.

Author contributions to the study and manuscript preparation include the following. Conception and design: Jeanmonod, Werner, Morel, Michels, Zadicario, Martin. Acquisition of data: Jeanmonod, Werner, Morel, Michels, Schiff, Martin. Analysis and interpretation of data: Jeanmonod, Morel, Michels, Schiff, Martin. Drafting the article: Jeanmonod, Morel, Michels. Critically revising the article: all authors. Reviewed submitted version of manuscript: Jeanmonod, Werner, Morel, Zadicario, Schiff, Martin. Approved the final version of the manuscript on behalf of all authors: Jeanmonod. Statistical analysis: Morel, Michels. Administrative/technical/material support: Jeanmonod, Zadicario, Schiff, Martin. Study supervision: Jeanmonod, Martin.

Acknowledgments

The authors are most grateful for the technical support of InSightec, Ltd. They thank M. Gallay and A. Poveda-Ramos for intraoperative patient monitoring and support.

References

1. Bourgeois G, Magnin M, Morel A, Sartoretti S, Huisman T, Tuncdogan E, et al: Accuracy of MRI-guided stereotactic thalamic functional neurosurgery. **Neuroradiology 41:**636–645, 1999
2. Chen L, Bouley D, Yuh E, D'Arceuil H, Butts K: Study of focused ultrasound tissue damage using MRI and histology. **J Magn Reson Imaging 10:**146–153, 1999
3. Chung AH, Jolesz FA, Hynynen K: Thermal dosimetry of a focused ultrasound beam in vivo by magnetic resonance imaging. **Med Phys 26:**2017–2026, 1999
4. Clement GT, Hynynen K: Correlation of ultrasound phase with physical skull properties. **Ultrasound Med Biol 28:**617–624, 2002
5. Clement GT, Hynynen K: Micro-receiver guided transcranial beam steering. **IEEE Trans Ultrason Ferroelectr Freq Control 49:**447–453, 2002
6. Clement GT, Hynynen K: A non-invasive method for focusing ultrasound through the human skull. **Phys Med Biol 47:**1219–1236, 2002
7. Clement GT, Sun J, Giesecke T, Hynynen K: A hemisphere array for non-invasive ultrasound brain therapy and surgery. **Phys Med Biol 45:**3707–3719, 2000
8. Clement GT, White J, Hynynen K: Investigation of a large-area phased array for focused ultrasound surgery through the skull. **Phys Med Biol 45:**1071–1083, 2000
9. Clement GT, White PJ, King RL, McDannold N, Hynynen K: A magnetic resonance imaging-compatible, large-scale array for trans-skull ultrasound surgery and therapy. **J Ultrasound Med 24:**1117–1125, 2005
10. Cohen ZR, Zaubermann J, Harnof S, Mardor Y, Nass D, Zadicario E, et al: Magnetic resonance imaging-guided focused ultrasound for thermal ablation in the brain: a feasibility study in a swine model. **Neurosurgery 60:**593–600, 2007
11. Connor CW, Clement GT, Hynynen K: A unified model for the speed of sound in cranial bone based on genetic algorithm optimization. **Phys Med Biol 47:**3925–3944, 2002
12. Hynynen K, Clement GT, McDannold N, Vykhodtseva N, King R, White PJ, et al: 500-element ultrasound phased array system for noninvasive focal surgery of the brain: a preliminary rabbit study with ex vivo human skulls. **Magn Reson Med 52:**100–107, 2004
13. Hynynen K, Jolesz FA: Demonstration of potential noninvasive ultrasound brain therapy through an intact skull. **Ultrasound Med Biol 24:**275–283, 1998
14. Hynynen K, McDannold N, Clement G, Jolesz FA, Zadicario E, Killiany R, et al: Pre-clinical testing of a phased array ultrasound system for MRI-guided noninvasive surgery of the brain—a primate study. **Eur J Radiol 59:**149–156, 2006
15. Hynynen K, Vykhodtseva NI, Chung AH, Sorrentino V, Colucci V, Jolesz FA: Thermal effects of focused ultrasound on the brain: determination with MR imaging. **Radiology 204:** 247–253, 1997
16. Jagannathan J, Sanghvi NT, Crum LA, Yen CP, Medel R, Dumont AS, et al: High-intensity focused ultrasound surgery of the brain: part 1—A historical perspective with modern applications. **Neurosurgery 64:**201–211, 2009
17. Jeanmonod D, Magnin M, Morel A: Low-threshold calcium

spike bursts in the human thalamus. Common physiopathology for sensory, motor and limbic positive symptoms. **Brain 119:**363–375, 1996
18. Jeanmonod D, Magnin M, Morel A: A thalamic concept of neurogenic pain, in Gebhart GF, Hammond DL, Jensen TS (eds): **Proceedings of the 7th World Congress on Pain. Progress in Pain Research and Management, Vol 2.** Seattle: International Association for the Study of Pain, 1994, pp 767–787
19. Jeanmonod D, Magnin M, Morel A, Siegemund M: Surgical control of the human thalamocortical dysrhythmia: I. Central lateral thalamotomy in neurogenic pain. **Thalamus Relat Syst 1:**71–79, 2001
20. Jeanmonod D, Morel A: The central lateral thalamotomy for neuropathic pain, in Lozano AM, Gildenberg Pl, Tasker RR (eds): **Textbook of Stereotactic and Functional Neurosurgery, ed 2.** Berlin: Springer-Verlag, 2009, pp 2081–2096
21. Jolesz FA, Hynynen K, McDannold N, Tempany C: MR imaging-controlled focused ultrasound ablation: a noninvasive image-guided surgery. **Magn Reson Imaging Clin N Am 13:** 545–560, 2005
22. Jolesz FA, McDannold N: Current status and future potential of MRI-guided focused ultrasound surgery. **J Magn Reson Imaging 27:**391–399, 2008
23. McDannold N, Clement GT, Black P, Jolesz F, Hynynen K: Transcranial magnetic resonance imaging-guided focused ultrasound surgery of brain tumors: initial findings in 3 patients. **Neurosurgery 66:**323–332, 2010
24. McDannold N, King RL, Hynynen K: MRI monitoring of heating produced by ultrasound absorption in the skull: in vivo study in pigs. **Magn Reson Med 51:**1061–1065, 2004
25. McDannold N, Vykhodtseva N, Jolesz FA, Hynynen K: MRI investigation of the threshold for thermally induced blood-brain barrier disruption and brain tissue damage in the rabbit brain. **Magn Reson Med 51:**913–923, 2004
26. Martin E, Jeanmonod D, Morel A, Zadicario E, Werner B: High-intensity focused ultrasound for noninvasive functional neurosurgery. **Ann Neurol 66:**858–861, 2009
27. Morel A: **Stereotactic Atlas of the Human Thalamus and Basal Ganglia.** New York: Informa Healthcare, 2007
28. Sarnthein J, Stern J, Aufenberg C, Rousson V, Jeanmonod D: Increased EEG power and slowed dominant frequency in patients with neurogenic pain. **Brain 129:**55–64, 2006
29. Schulman JJ, Ramirez RR, Zonenshayn M, Ribary URS, Llinas R: Thalamocortical dysrhythmia syndrome: MEG imaging of neuropathic pain. **Thalamus Relat Syst 3:**33–39, 2005
30. Stern J, Jeanmonod D, Sarnthein J: Persistent EEG overactivation in the cortical pain matrix of neurogenic pain patients. **Neuroimage 31:**721–731, 2006
31. Sun J, Hynynen K: The potential of transskull ultrasound therapy and surgery using the maximum available skull surface area. **J Acoust Soc Am 105:**2519–2527, 1999
32. Vykhodtseva NI, Sorrentino V, Jolesz FA, Bronson RT, Hynynen K: MRI detection of the thermal effects of focused ultrasound on the brain. **Ultrasound Med Biol 26:**871–880, 2000

Manuscript submitted September 15, 2011.
Accepted October 27, 2011.
Please include this information when citing this paper: DOI: 10.3171/2011.10.FOCUS11248.

Address correspondence to: Daniel Jeanmonod, M.D., Center of Ultrasound Functional Neurosurgery, Leopoldstrasse 1, 4500 Solothurn, Switzerland. email: daniel.jeanmonod@gmail.com.